33

Bio-inspired Interaction Control of Robotic Machines for Motor Therapy

Loredana Zollo, Domenico Formica, Eugenio Guglielmelli
Laboratory of Biomedical Robotics & EMC, Campus Bio-Medico University,
Via Emilio Longoni 83, 00155 Rome, Italy

1. Introduction

The idea of robot-aided motor therapy was first introduced in the early 1990s (Khalili & Zomlefer, 1988), (Hogan et al., 1992), and is gaining an increasing popularity. Many different platforms have been developed worldwide (Krebs et al., 1998), (Colombo et al., 2000), (Lum et al., 1999), (Reinkensmeyer et al., 2000a), (Kiguchi & Fukuda, 2004), (Costa et al., 2004), and some commercial systems appeared on the market sustained by encouraging, though still limited results of clinical trials.

The design and the production of devices for application in robot-aided motor therapy requires a multidisciplinary group, composed of neuroscientists, physiatrists, therapists and bioengineers, that strictly collaborate for the definition of the functional specifications of the machine, so that neurophysiological requirements are fulfilled and the artificial system and the natural system are integrated as functional and less invasive as possible.

A crucial design challenge in robot-aided rehabilitation is interaction control between the robotic machine, the patient, and the therapist. That is because the machine has to permanently operate in a constrained motion, where a direct mechanical coupling always exists between the patient (or the limb involved in the robotic treatment) and the machine (Reinkensmeyer et al., 2000b). Tight physical interaction between the robot and the human body is not occasional, like in many other industrial or service robotic applications, but it is an intrinsic functional requirement; moreover, the working environment can be regarded as partially unstructured, since interaction conditions between the robot and the patient can notably vary depending on the residual motor capabilities of patients and their unpredictable reactions to therapeutic stimuli.

The design and development of interaction control for rehabilitation robotic machines can resort to a wide range of control strategies derived from industrial robotics for managing human-machine physical interaction (Siciliano & Villani, 1999), (Gorinevsky et al., 1997), (Salisbury, 1980), (Kazerooni et al., 1986), (Zollo et al., 2003). Take for example impedance control (Hogan, 1985): it is successfully used in motor therapy (Krebs et al., 1998) as it allows finely regulating the mechanical impedance of robots interacting with unstructured environments. It is basically thought for interaction in the Cartesian space and, consequently, it is especially applicable to 'operational machines', where only the motion of the robot end-effector in the operational space (and not that of the robot joints in the joint space) is equivalent to that of the natural effector of the human limb - hand or foot.

Source: Rehabilitation Robotics, Book edited by Sashi S Kommu,
ISBN 978-3-902613-04-2, pp.648, August 2007, Itech Education and Publishing, Vienna, Austria

However, impedance control requires an accurate knowledge of the dynamic parameters of the robotic system, in order to compensate the robot dynamics. This increases difficulties in implementing the control law and entails computational burden which may limit the field of application of this powerful technique.
Thus, although applicable and adaptable to robot-aided motor therapy, control strategies derived from industrial robotics do not fully satisfy motor therapy requirements and substantial efforts are currently being devoted to robot design and control approaches purposely conceived for improving dependability in human-robot interaction (Formica et al., 2005), (Bicchi & Tonietti, 2004), (Zinn et al., 2004), (Colombo, 2004). Also biomorphic control techniques are being developed for such an application field that are inspired to recent neuroscientific findings on sensorimotor coordination and viscoelastic regulation in humans (Zollo et al., 2005), (Formica et al., 2006).
The control system of a machine for robot-aided neuro-rehabilitation is required to be highly **adaptable** and **safe**. In particular, the robot control system has to ensure a high level of adaptability to the different motor capabilities of the patients, properly relaxing the requirement of stiffness and precision in the motor task and remarking the maximum priority of safety in the interaction. Also, an ideal control system has to be **portable**, so to be easily instantiated on different types of rehabilitation machines, i.e., operational rehabilitation machines or else exoskeletal rehabilitation machines, still providing similar therapeutic performance by just readapting few parameters of the control law (Formica et al., 2005), (Micera et al., 2005).
Finally, a good level of **flexibility** is needed for the machine to be prone to implement different motor tasks, with various kinematic and dynamic characteristics as required by different clinical research protocols. In particular, studies on the typical tasks of rehabilitation motor therapy have shown that, in view of the differences in the patient residual motor capabilities, at least three different operating modalities can be listed which the control has to be able to implement (Krebs et al., 2003). They are:

- **Passive Mode**: the patient is unable to autonomously accomplish the motor task and the robot actively drives her/his limb. The trajectory is fully determined by the robot control system, unless the patients opposes a resistance to motion which exceeds Safety specifications;
- **Active-Assisted Mode**: the patients starts the movement but he/ she is unable to reach the target; the robot helps her/his complete the programmed task. When the robot takes control of the task, it goes to passive mode. Initially the machine is fully compliant to human motion, until it stops;
- **Active-Constrained Mode**: the patient is able to complete the movement, and the robot can exert a set of programmed force fields to allow a complete recovery of the muscular tone. Here, the trajectory of the end effectors dynamically depends on the interaction between the robot and the human limb.

This chapter proposes a control approach which tries to fulfil the requirements of adaptability, safety, portability, and flexibility derived from the application field of rehabilitation robotics and adopts a bio-inspired approach for regulating robot behavior in the interaction with the patient. It originates from the analysis of the basic operating modalities of the rehabilitation motor therapy and, also, from the study of the fundamental mechanisms of biological motor control for generating planar movements and viscoelastic regulation in the human arm (Mussa-Ivaldi et al., 1985), (Katayama & Kawato, 1993), (Gomi & Kawato, 1997), (Gomi & Osu, 1998), (Gomi, 1998).

Two bio-inspired compliance control laws for biomedical applications are presented in this chapter, which try to overcome limitations of the traditional interaction control. They are named *coactivation-based compliance control in the joint space* (Zollo et al., 2005), (Zollo et al., 2003), and *torque-dependent compliance control in the joint space* (Formica et al., 2006), (Formica et al., 2005), respectively. Both of them are compliant controls in the joint space, thus being computationally simple with respect to other traditional approaches and potentially applicable to operational as well as exoskeletal machines.
The *coactivation-based compliance control in the joint space* derives its name from the coactivation mechanism responsible of muscle visco-elastic regulation in the human arm and uses a unique parameter (purposely named coactivation) to modulate joint compliance in the interaction.
The *torque-dependent compliance control in the joint space* tries to mimic the action of the central nervous system in regulating elastic properties of the human arm. In particular, relation between torques exerted by muscles and joint stiffness is studied and replicated with a good approximation by the control in an inner loop. On the other hand, an outer loop is responsible for controlling human robot interaction by means of a traditional direct force control law.
Control theoretical formulation is presented in Sect. 2. Then, in Sect. 3 a comparative validation of basic adaptability and safety requirements of the two control schemes is carried out in simple and ordinary tasks, such as reaching and contact/noncontact transitions. The comparative analysis is performed in simulation tests, by means of a simulation tool purposively developed in MATLAB/Simulink for modeling interaction, and in experimental trials on an 8 degree-of-freedom (dof) robot arm. The preliminary experimental tests are reported to demonstrate the feasibility of using the proposed approach for guaranteeing safe interaction with the patient. Finally, Sect. 4 reports results of simulation tests of interaction between an operational machine and a patient in a plane during motor therapy. The dynamics of the MIT-Manus rehabilitation robotic machine (Krebs et al., 1998) is modelled as coupled with the dynamics of the human arm and a set of incorrect movements of the patient is generated within the simulation environment to test the control capability of counterbalancing a pathological behaviour.

2. Control theoretical formulation

Control for robotic machines for motor therapy can be regarded as interaction control for unstructured or partially unstructured environment, as interaction conditions are strongly dependent on the residual motor capabilities of patients. The control is also aiming to be highly adaptable, flexible and applicable to operational as well as exoskeletal machines.
The two control laws proposed in this work have been specifically conceived for this scenario and originate from the joint analysis of biological motor control (in particular human motor control of the upper limb) and robot interaction control in unstructured environment. They are the *coactivation-based compliance control in the joint space* (Zollo et al., 2005) and the *torque-dependent compliance control in the joint space* (Formica et al., 2006), respectively.
Concepts of muscular coactivation and joint stiffness regulation have been borrowed from neuroscience for improving robot performance in situations of interaction with an unstructured environment and, particularly, in contact/noncontact transitions. To this purpose, the control laws take into account the two cases of motion in the free space and

motion in the constrained space and a bio-inspired approach is proposed to control interaction force and accuracy by feedback.
Furthermore, as already explained in (Zollo et al., 2003 a), (Zollo et al., 2005) the choice of designing an interaction control based on the compliance regulation at the level of joint space is entailed by several factors. From neurophysiological studies (Mussa-Ivaldi et al., 1985), (Katayama & Kawato, 1993), (Gomi & Kawato, 1997), (Gomi & Osu, 1998), (Gomi, 1998), (Osu & Gomi, 1999), it emerges that visco-elastic regulation in humans is directly achieved at the level of muscles and joints and indirectly at the level of end effector. On the other hand, from a robot control viewpoint, implementing a control in the joint space does not require to enter details of robot dynamics, thus allowing reducing the computational burden and extending the approach to different mechanics. This implies that in applications of rehabilitation motor therapy a control in the joint space can be easily applied to operational as well as exoskeletal machines.

2.1 Coactivation-based compliance control in the joint space

The coactivation-based compliance control law (Zollo et al., 2005) borrows from biology the term coactivation, that is the biological mechanism responsible for the regulation of the arm viscoelastic properties at the level of muscles and joints, and indirectly at the level of end effector (Katayama et al., 1998) (Baldissera 1981), (Serres & Milner, 1991). Moreover, in (Katayama et al., 1998) it is proposed that in the human arm feedback acts in the interaction control by regulating the muscular activity in accordance with the movement error.
The coactivation-based compliance control law is formulated as follows (Zollo et al., 2005):

$$\tau = K_P(c)\tilde{q} - K_D(c)\dot{q} + g(q) \tag{1}$$

where $g(q)$ is the estimate of the gravitational torques acting on the joints, and stiffness and damping matrices K_P and K_D are linear functions of a unique parameter c, called coactivation by analogy with the biological mechanism.
An appropriate choice for the *c* function allows improving arm accuracy in free space, by increasing stiffness, and increase arm compliance and elasticity in constrained space, by decreasing stiffness when an external bound is sensed. In both cases, the gains of diagonal matrices K_P and K_D evolve from an initial value, experimentally evaluated, as a function of a unique factor, that is the coactivation.
In the free space, the *i*-th element of K_P increases from its minimum value as:

$$k_P(c) = \begin{cases} k_{p\min} & if\ \ c = 0 \\ k_{P\min} + \bar{k}_p c & if\ \ c \neq 0, k_P < k_{P\max} \\ k_{P\max} & if\ \ c \neq 0, k_P \geq k_{P\max} \end{cases} \tag{2}$$

where the coefficient $\bar{k}_P$ can be different for each joint, in order to allow regulating the level of coactivation for each of them. In (2), $k_{P\min}$ is the minimum gain allowing a quite accurate motion and $k_{P\max}$ is the maximum gain which still ensures stability in the motion. The updating law for c is an increasing monotonic function of the sole position error, i.e.

$$c = \beta\sqrt{\tilde{q}^T\tilde{q}} \tag{3}$$

as presented in (Katayama et al., 1998) for the human visco-elastic regulation. In (3), β is a positive coefficient. An analogous adaptable law is proposed for the viscosity parameters. The *i*-th element of K_D matrix evolves over time like (2), but with a slower increasing rate, i.e.,

$$k_D(c) = \begin{cases} k_{D\min} & if\ \ c = 0 \\ k_{D\min} + \bar{k}_d c & if\ \ c \neq 0, k_D < k_{D\max} \\ k_{D\max} & if\ \ c \neq 0, k_D \geq k_{D\max} \end{cases} \tag{4}$$

In the constrained space, k_P function decreases with the force module from its initial value k_{Pin}

$$k_P(c) = k_{Pin}\bar{h}c \tag{5}$$

$$c = c_{\min} + \alpha\frac{1}{\sqrt{f^T f}} \qquad if \quad f^T f \neq 0 \tag{6}$$

where $k_{Pin}\bar{h}$ is the maximum value for the proportional parameter, and $\bar{h}$ is a scalar coefficient playing the same role of $\bar{k}_P$. The viscosity parameters k_D in constrained motion observes the same law as in (5).

The block scheme of the *coactivation-based compliance control in the joint space* is reported in Fig. 1.

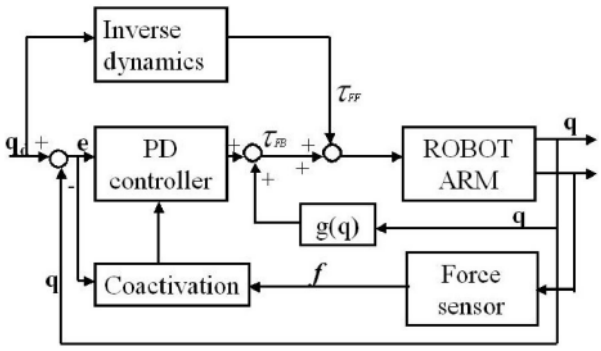

Fig. 1. Block scheme of the coactivation-based compliance control.

2.2 Torque-dependent compliance control in the joint space

In the human arm, joint stiffness seems To be strictly dependent on the torques exerted by the muscles on the joints. In particular, joint stiffness seems to increase as the torque module raises, as shown in Fig. 2 extracted from (Gomi & Osu, 1998).

The *torque-dependent compliance control in the joint space* is a parallel force/position control where the position control is a compliance control in the joint space based on PD actions.

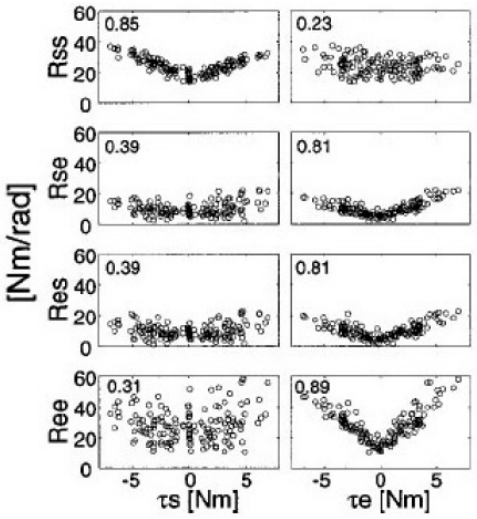

Fig. 2. Joint torque and joint stiffness relationships for one subject (extracted from Gomi & Osu, 1998).

In the free space the PD control tries to replicate results obtained in (Gomi & Osu, 1998) on human subjects, by making the joint stiffness linearly vary with the torque module as:

$$R_{ij}(\tau_k^m) = \begin{cases} R_{ij}^{\min} + k_{ij}\left|\tau_k^m\right| & if \;\; R_{ij} < R_{ij}^{\max} \\ R_{ij}^{\max} & if \;\; R_{ij} \geq R_{ij}^{\max} \end{cases} \tag{7}$$

where $i, j, k = \{e, s\}$, being subscripts e and s the elbow and shoulder joint, respectively. Note that a maximum value $R_{ij}^{\max}$ for each joint needs to be imposed in order to avoid instability in the control.
The corresponding stiffness matrix is:

$$R(\tau^m) = \begin{bmatrix} R_{ss}(\tau_s^m) & R_{se}(\tau_e^m) \\ R_{es}(\tau_e^m) & R_{ee}(\tau_e^m) \end{bmatrix}. \tag{8}$$

As regards damping matrix D, it is assumed to be constant since in (Gomi & Osu, 1998) the variation of viscosity with joint torques seems to be negligible.
Finally, in the free space robot behavior is regulated by the following control law:

$$\tau = R(\tau^m)\tilde{q} - D\dot{q} + g(q) \tag{9}$$

being $R(\tau^m)$ defined in (7) and (8).
For the robot behaviour in the interaction with the human subject, the traditional approach to force control (Siciliano & Villani, 1999) is used. This is because the control is thought to be applied to motor therapy, where the three modalities of passive mode, active assisted mode and active constrained mode are to be performed.

Thus, the basic idea for the control in the interaction with a patient is that the therapist is capable of guiding, assisting or forcing the subject in the execution of the motor task. Control in the constrained space is then based on a force feedback loop which, in addition to a position loop, makes the robot capable of changing the desired trajectory depending on the force error (Fig. 3).
The desired trajectory the robot has to follow in the Cartesian space is composed of two terms:

$$x_d = x_{dp} + x_F \tag{10}$$

where x_{dp} is the desired trajectory in absence of interaction, and x_F determines the displacement from x_{dp} depending on the force error. Vector x_F is calculated as follows:

$$x_F = K_{FP}(F_d - F) + K_{FI}\int_0^t (F_d - F)d\zeta \cdot \tag{11}$$

In (11) K_{PF} and K_{FI} are the proportional and integral gain matrices of the force control and F_d is the reference force vector set by the robot user.
The block scheme of the *torque-dependent compliance control in the joint space* is shown in Fig. 3.

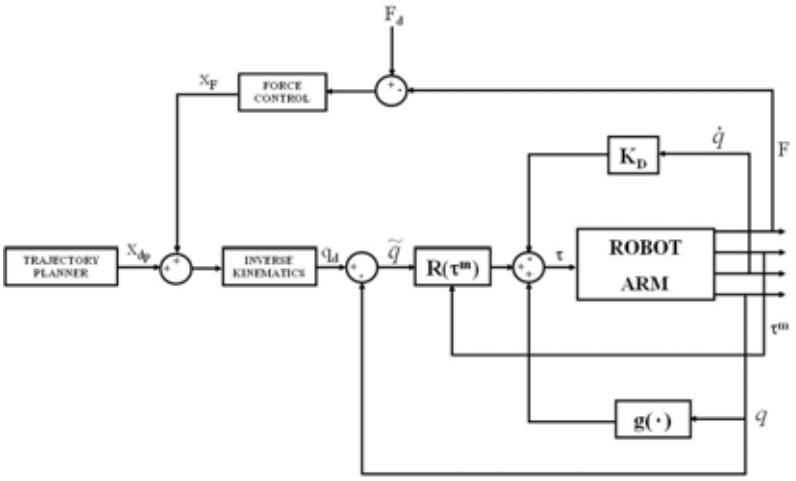

Fig. 3. Block scheme of the torque-dependent compliance control.

3. Comparative analysis of the proposed control schemes

3.1 Description of the simulation tool

A simulator has been developed in MATLAB/Simulink for a preliminary validation and a comparative analysis of the control laws (1) and (9). The simulator models a 2-dof robot arm interacting with a human arm (Formica et al., 2005), (Formica et al., 2006).
The simulated robot arm is the 2-dof MIT-Manus operational robotic machine (see Fig. 4). The main reason for the choice of the MIT-Manus system is that it is a commercial robot

specifically designed for robot-aided rehabilitation and tested in several clinical studies on motor therapy (Krebs et al., 1998), (Krebs et al., 1999), (Krebs et al., 2000), (Fasoli et al., 2003). The model developed in MATLAB/Simulink is based on kinematic and dynamic parameters extracted from (Bhushan & Shadmehr, 1999).
On the other hand, for the human arm a simplified planar model has been considered, consisting of two joints (a shoulder and an elbow), two links and three couples of muscles (see Fig. 4) (Katayama & Kawato, 1993). This type of simplified model is widely used in most neurophysiological studies regarding human motor control (Hogan, 1985), (Miall, 1998).

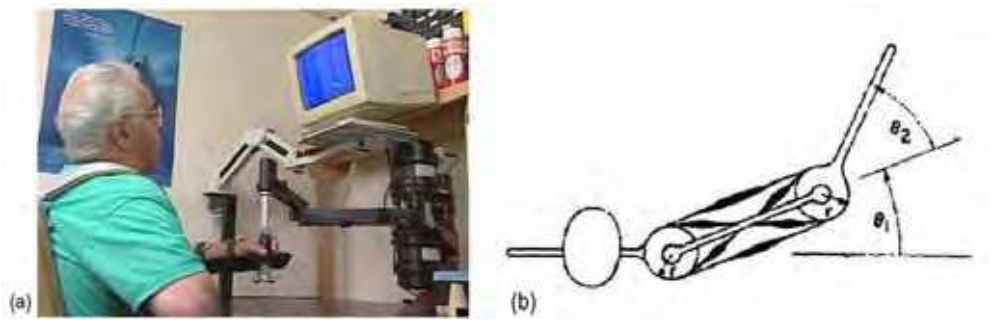

Fig. 4. The MIT-Manus rehabilitation robot (a), and a planar model of the human arm (b).

The dynamic model of the MIT-Manus robot can be described as:

$$B_{ROB}(q)\ddot{q} + C_{ROB}(q,\dot{q})\dot{q} = \tau_{ROB} - J_{ROB}^{T}(q)F_{ROB} \tag{12}$$

whereas the dynamics of the human arm interacting with the robot can be expressed as:

$$B_{HUM}(\theta)\ddot{\theta} + C_{ROB}(\theta,\dot{\theta})\dot{\theta} = \tau_{HUM} - J_{HUM}^{T}(\theta)F_{HUM} \tag{13}$$

In (12) and (13),

- $q, \dot{q}, \ddot{q} \in R^{2\times1}$ are the robot joint position, velocity and acceleration vectors, respectively;
- $B(q) \in R^{2\times2}$ is the joint inertia matrix;
- $C(q,\dot{q})\dot{q} \in R^{2\times1}$ is the vector of centrifugal and Coriolis torques;
- $J(q) \in R^{2\times2}$ is the robot Jacobian matrix;
- $\tau \in R^{2\times1}$ is the torque vector;
- $F \in R^{2\times1}$ is the vector of forces exerted on the external environment;

and subscripts ROB and HUM indicate that the quantities are referred to the MIT-Manus and the human arm, respectively.
Numerical values for matrices $B_{ROB}(q)$, $C_{ROB}(q,\dot{q})$, and $J_{ROB}(q)$ are taken from (Bhushan & Shadmehr, 1999), while for $B_{HUM}(q)$, $C_{HUM}(q,\dot{q})$, $J_{HUM}(q)$ anthropometric data in (Katayama & Kawato, 1993) are used.
Furthermore, in view of the physical interaction between the two systems, forces F_{ROB} and F_{HUM} are equal in module and opposite in sign (i.e., $F_{ROB} = -F_{HUM}$) whereas position, velocity and acceleration in the Cartesian space are the same. The inequality between kinematic variables yields

$$\theta = k_{HUM}^{-1}[k_{ROB}(q)] \tag{14}$$

$$\dot{\theta} = J_{HUM}^{-1}(\theta) J_{ROB}(q)\dot{q} \tag{15}$$

$$\ddot{\theta} = J_{HUM}^{-1}(\theta)[\dot{J}_{ROB}(q)\dot{q} + J_{ROB}(q)\ddot{q} - \dot{J}_{HUM}(\theta)\dot{\theta}] \tag{16}$$

being $k_{ROB}(q)$ the robot forward kinematics and k_{HUM}^{-1} the inverse kinematics of the human arm, and joint variables for the human arm (i.e., $\ddot{\theta}, \dot{\theta}, \theta$) can be calculated as a function of the MIT-Manus joint variables (i.e., $q, \dot{q}, \ddot{q}$).

By substituting Eqs. (14)-(16) in (13) and extracting $F_{HUM} = -F_{ROB}$, a complete dynamic model of the interacting human-robot system can be obtained through Eq. (12).

In Fig. 5 the image of the two simulated interacting systems is shown. The MIT-Manus system is represented in blue while the human arm is in red. The handle of the robot where the patient is attached is coloured in pink.

Control torques τ_{ROB} for the robotic system are provided by the robot control law.

For the human arm, instead, motor torques τ_{HUM} are generated by the motor commands from the CNS (Katayama & Kawato, 1993), (Hogan, 1985), (Miall, 1998) and depend on the visco-elastic muscle behaviour. Here, for sake of simplicity, human muscular activity is not modelled and only the consequence at the level of joints is considered. This entails a joint visco-elastic behavior described as:

$$\tau_{HUM} = R_{HUM}(\theta_d - \theta) - D_{HUM}\dot{\theta} \tag{17}$$

where the values of joint stiffness matrix R_{HUM} and damping matrix D_{HUM} have been resumed from the human data on the joint visco-elastic parameters in (Gomi & Osu, 1998). Vector θ_d is the arm desired trajectory in the joint space.

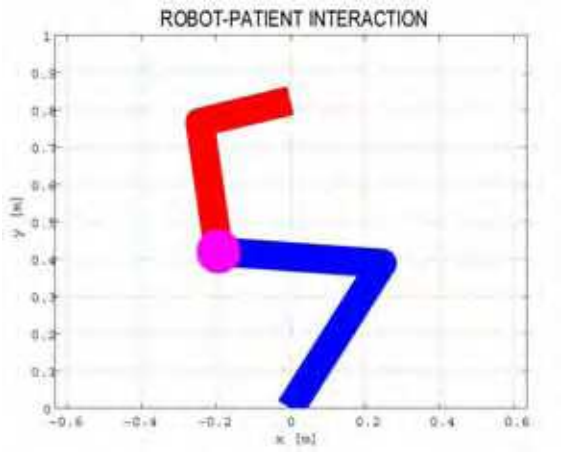

Fig. 5. Graphical interface of an operational robotic machine interacting with a human subject: the MIT-Manus robot arm is drawn in blue, the human arm is drawn in red.

3.2 Simulation results

Performance of the coactivation-based compliance control in the joint space and of the torque-dependent compliance control in the joint space have been preliminarily compared

through the developed simulation tool. The robot arm is regarded as an uncoupled system (i.e., without coupling with the human subject) and is controlled to execute motor tasks of positioning in the free space as well as of interaction with an unexpected constraint.

For the simulation tests in the free space, the robot arm is moved in the Cartesian space from the initial position $P_i = [-0.2; 0.58]$ m to the final position $P_f = [0.2; 0.58]$ m in 4s plus 2s for the adjustment.

For the control law (1) the gains have been chosen as: $K_{P\min} = \text{diag}\{10.8 \cdot 40,\ 8.67 \cdot 40\}$ Nm/rad, $\overline{K}_P = \{2.86 \cdot 40,\ 6.82 \cdot 40\}$ Nm/rad, $K_{D\min} = \text{diag}\{4,\ 4\}$ Nm/rad·s^{-1}, $\overline{K}_d =$ diag{0.1, 0.1} Nm/rad·s^{-1}, $\beta = 50$. On the other hand, for control (9) the visco-elastic parameters have been set as: $R_{ss}^{\min} = 10.8 \cdot 40$ Nm/rad, $R_{ee}^{\min} = 8.67 \cdot 40$ Nm/rad, $R_{se}^{\min} = 2.15 \times 40$ Nm/rad, $R_{ss}^{\min} = 2.34 \cdot 40$ Nm/rad, $k_{ss} = 2.86 \cdot 40$ rad^{-1}, $k_{ee} = 6.82 \cdot 40$ rad^{-1}, $k_{se} = k_{es} = 7.5 \cdot 40$ rad^{-1}, and $D =$ diag{4, 4} Nm/rad·s^{-1}.

The norm of the position error in the Cartesian space for the two cases of coactivation-based compliance control and torque-dependent compliance control is shown in Figs. 6 and 7, respectively. The error time course is very similar and in both cases the maximum value is close to $1.3 \cdot 10^{-3}$ m.

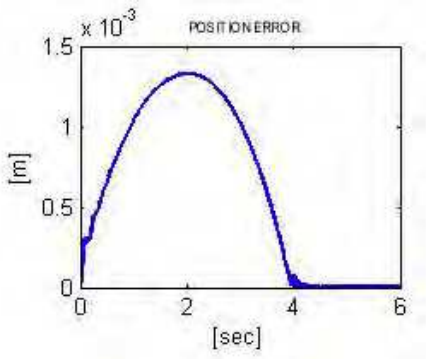

Fig. 6. Simulation results on position error in the free space for the coactivation-based compliance control law.

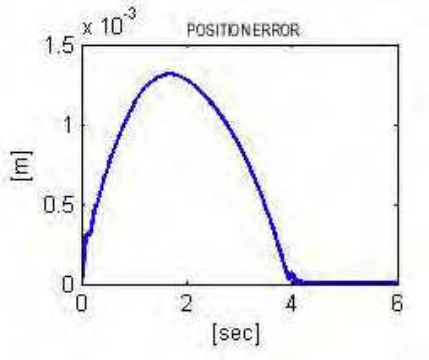

Fig. 7. Simulation results on position error in the free space for the torque-dependent compliance control law.

For simulating an unexpected interaction with the environment, an external constraint is modelled as an elastically compliant system having stiffness K_e and described by the following equation:

$$F_e = K_e(x_e - x) \tag{18}$$

being x_e and x the Cartesian position of the constraint and the robot end effector, respectively.

The robot is moved from the initial position P_i=[0.46; 0.44] m to the final position P_f=[−0.46; 0.44] m, and the obstacle is assumed to be vertically positioned in x_e=−0.2 m (K_e is set to 10^4 N/m). Figures 8 and 9 report the interaction force in norm for the two cases of coactivation-based and torque-dependent compliance control.

In order to compare force performance, control gains for the two control laws have been tuned to generate the same position error. As evident, the interaction force related to (1) presents a series of spikes in the contact/noncontact transition phase which are notably reduced in number and amplitude for the control (9). After the transient, both controllers adapt to the constraint and reach a reasonable force value, that is close to *5* N for the controller (1) and *1* N for the controller (9).

In the constrained motion, the control gains of the coactivation-based control law in (5), (6) are chosen as: K_{Pin}=diag{40, 8} Nm/rad, $\overline{H}$ =diag{0.8, 0.7}, c_{min}=0.4, α=1. For the force control in (11) control gains have the following values: K_{FP}=10^{-3} mN^{-1}, K_{FI}=10^{-2} m $(Ns)^{-1}$.

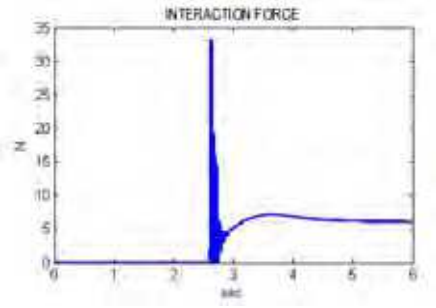

Fig. 8. Simulation results on interaction force in the constrained motion for the coactivation-based compliance control law.

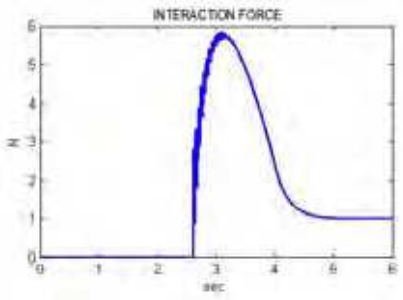

Fig. 9. Simulation results on interaction force in the constrained motion for the torque-dependent compliance control law.

3.3 Experimental results

Experimental trials of reaching in the free space and motion in the constrained space have been carried out to complete the compared evaluation of the two control laws.
The experimental robotic platform consists of the Dexter arm, a robot manipulator at the ARTS Lab of the Scuola Superiore Sant'Anna of Pisa and manufactured by Scienzia Machinale s.r.l. for applications of assistive robotics, and a six-axis ATI force/torque sensor (see Fig. 10).
The Dexter arm is made of 8 rotational joints actuated by a mechanical transmission system of pulleys and steel cables which determines coupling in the degrees of freedom (see (Zollo et al., 2003 b) for further details). The force/torque sensor is mounted at the arm wrist and is capable of reading force in the range of [−210, +210]N.

The sensor is used to monitor force values during interaction and close the loop in the force control. A photo of the experimental setup is shown in fig. 10.

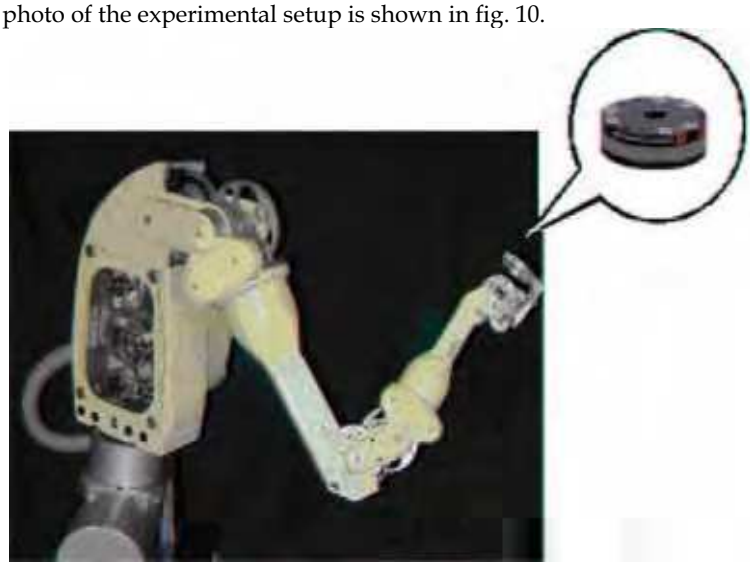

Fig. 10. The Dexter robot arm with the force sensor mounted on the arm wrist.

The control law is written in C++ programming language and run on a PC Pentium II under DOS Operating System. The motor commands are sent to the actuation system every 10 ms, by means of two MEI 104/DSP-400 control boards.
As in the simulated environment, the experimental tests consist of a series of point-to-point movements in the free space as well as in the constrained space.
For tests in the free space, the Dexter arm is moved in the Cartesian space from the initial position P_i = [0.70;−0.25; 0.50] m to the final position P_f=[0.50; 0.25; 0.45] m in 13 s plus 3 s for the adjustment. A point-to-point quintic polynomial trajectory (with zero velocity and acceleration boundary conditions) has been planned to guide the robot from the initial to the final configuration. The experimental tests have been performed with high gain values, in order to reach the target position with high precision. Thus, for the coactivation-based compliance control, the following values have been chosen: K_{Pmin} =diag{60, 40, 10, 9, 8, 1, 0.2, 0.2} Nm/rad, β= 1.5, $\overline{K}_P$ =diag{3, 2.5, 2.5, 2, 1.8, 1, 0.2, 0.2} Nm/rad.

Instead, for the torque-dependent compliance control R_{min}=diag{640, 120, 80, 64, 32, 4, 4} Nm/rad, k=diag{20, 20, 16, 14.4, 8, 4, 4} rad^{-1} and K_D=diag{10, 10, 6, 2, 2, 0.8, 0.8} Nm/rad ·s^{-1} have been set.
The position error in the Cartesian space is shown in Figs. 11 and 12, respectively. Definitely, in the free space performance of the two compliance control laws seems to be comparable.

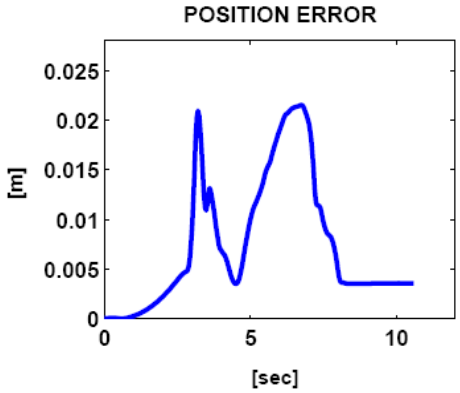

Fig. 11. Experimental results: norm of the position error in the free space for the coactivation-based compliance control.

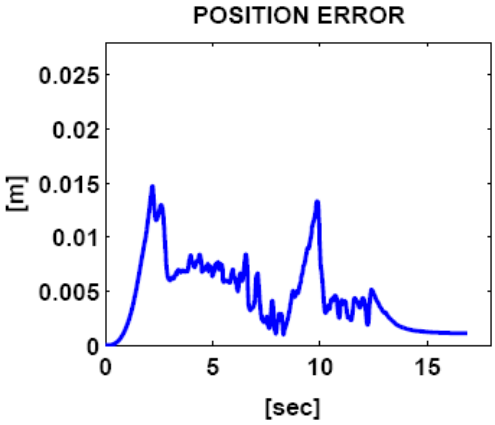

Fig. 12. Experimental results: norm of the position error in the free space for the torque-dependent compliance control.

To evaluate the adaptability of the control laws to unexpected constraints, the robot arm has been commanded to move from the initial position P_i = [0.50; 0; 0.40] m to the final position P_f = [0.75; 0; 0.40] m and the experimenter is instructed to constrain the robot end effector by using his/her hand at about x = 0.60 m.
The results shown in Figs. 13, 14 correspond to the following set of control parameters: K_{Pin} =diag{60, 40, 15, 10, 8, 4, 1, 1} Nm/rad, $\overline{H}$ =diag{1, 0.8, 0.8, 0.7, 0.7, 0.5, 0.1, 0.1}, c_{min} = 0.4, β=1 for the control law (1) and K_{FP} = 10^{-3} mN^{-1}, K_{FI} = 10^{-2} m (Ns)$^{-1}$, F_{dx}=−5 N, F_{dy}=F_{dz}=0 N

for the control law (9). In both cases the robot adapts the trajectory to the external constraint and, for the control (9) it also regulates the interaction force to the desired value. However, it is worth noticing that for the second controller, i.e. the torque-dependent compliance control, force time course never resulted in sharp variations at the impact with the constraint, whereas for the coactivation-based compliance control force time course appears to be quite impulsive in the adaptation to the obstacle (Fig. 13). This achievement is in accordance with results in Figs. 8 and 9 obtained in the simulation tests and is extremely important for selecting the appropriate control law for biomedical applications, where safety and smooth adaptability in the interaction with humans are requirements with maximum priority.

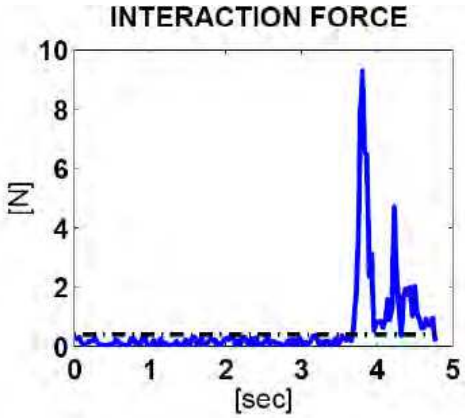

Fig. 13. Experimental results: interaction force in the constrained motion for the coactivation-based compliance control law.

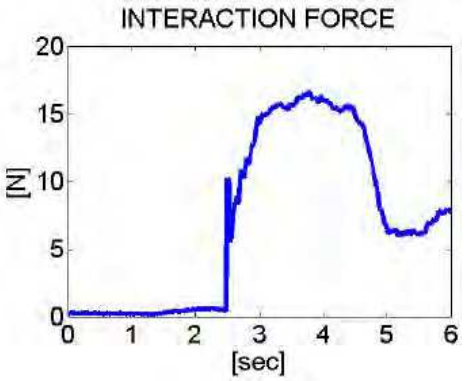

Fig. 14. Experimental results: interaction force in the constrained motion for the torque-dependent compliance control law.

4. Simulation tests of human-robot interaction during motor therapy

Following the results of the comparative analysis between the two control laws, which clearly indicate the torque-dependent compliance control to be the safer and

more adaptable with respect to the coactivation-based compliance control, an application of (9) to interaction with a patient during tasks of motor therapy has been simulated.

In particular, through the simulator presented in Sect. 3.1 three different levels of motor disabilities have been modelled, in order to test system adaptability to different motor conditions of patients. For simplicity, the different pathological levels have been represented by means of sharp deviations of the human arm from the linear reference trajectory. Whereas a linear motion from a generic point A to a point B is expected for a healthy subject, a sequence of short linear paths (like a sawtooth function) can be roughly imagined for a patient undergoing neurorehabilitation therapy. The rate of variation of the sawtooth is assumed to be dependent on the level of disability.

The MIT-Manus robot arm is controlled to linearly move from the initial point P_i=[−0.20; 0.42] m to the final point P_f = [0.20; 0.42] m in 4 s and force the patient to follow a linear motion in accordance with the level of disability. As natural, the level of robot force has to be opportunely tuned to guarantee safety of operation with human subjects.

To this purpose, the reference value for the force control consists of two contributions:

- A force F_{dx}=const that guides the arm in the direction of motion;
- A force perpendicular to the motion direction which counterbalances incorrect movements. It is expressed as $F_{dy} = K_y \cdot \tilde{y}$, where $\tilde{y}$ is the position error in the direction perpendicular to the motion and gain K_y assumes higher values as the level of disability increases.

Table 1 reports the values of the parameters of the force control used for simulating interaction in the three cases of disability.

Disability Level1	Disability Level 2	Disability Level3
F_{dx}=5 N	F_{dx}=15 N	F_{dx}=30 N
K_y=100 N/m	K_y=100 N/m	K_y=100 N/m
F_{dx}=15 N	F_{dx}=30 N	F_{dx}=45 N
K_y=100 N/m	K_y=100 N/m	K_y=100 N/m
F_{dx}=5 N	F_{dx}=15N	F_{dx}=30 N
K_y=1000 N/m	K_y=1000 N/m	K_y=1000 N/m
F_{dx}=15 N	F_{dx}=30 N	F_{dx}=45 N
K_y=1000 N/m	K_y=1000 N/m	K_y=100 N/m

Table 1. Parameters for the force control in the simulation tests of robot interacting with the patient.

For brevity, simulation results only for two levels of disability are reported here. They are shown in Figs. 15 and 16 and correspond to the simulated Cases of slight (Level 1) and severe disability (Level 3), respectively. The two figures show the incorrect movements executed by the patient in absence of the MIT-Manus assistance and the movement described by the patient when guided by the robot.

The efficacy of robot corrective actions directly depends on F_{dx} and, especially, on K_y. This is evident also in the case of severe disability shown in Fig. 16.

However, it is worth noticing that the value of the control parameters is superiorly limited due to insurgence of instability and problems of safety in the interaction. High values may determine interaction force that can be dangerous for the patient. For instance, when the

critical case of severe disability and high control parameters (F_{dx}=*45 N*, K_y=*1000 N/m*) has been simulated the interaction force has reached a dangerous peak value of nearby *80 N* (see Fig. 17). Therefore, a superior limit needs to be imposed to the force exerted by the robot while guiding the human arm, that is around *45–50* N as for the real MIT-Manus system (Krebs et al., 1998).

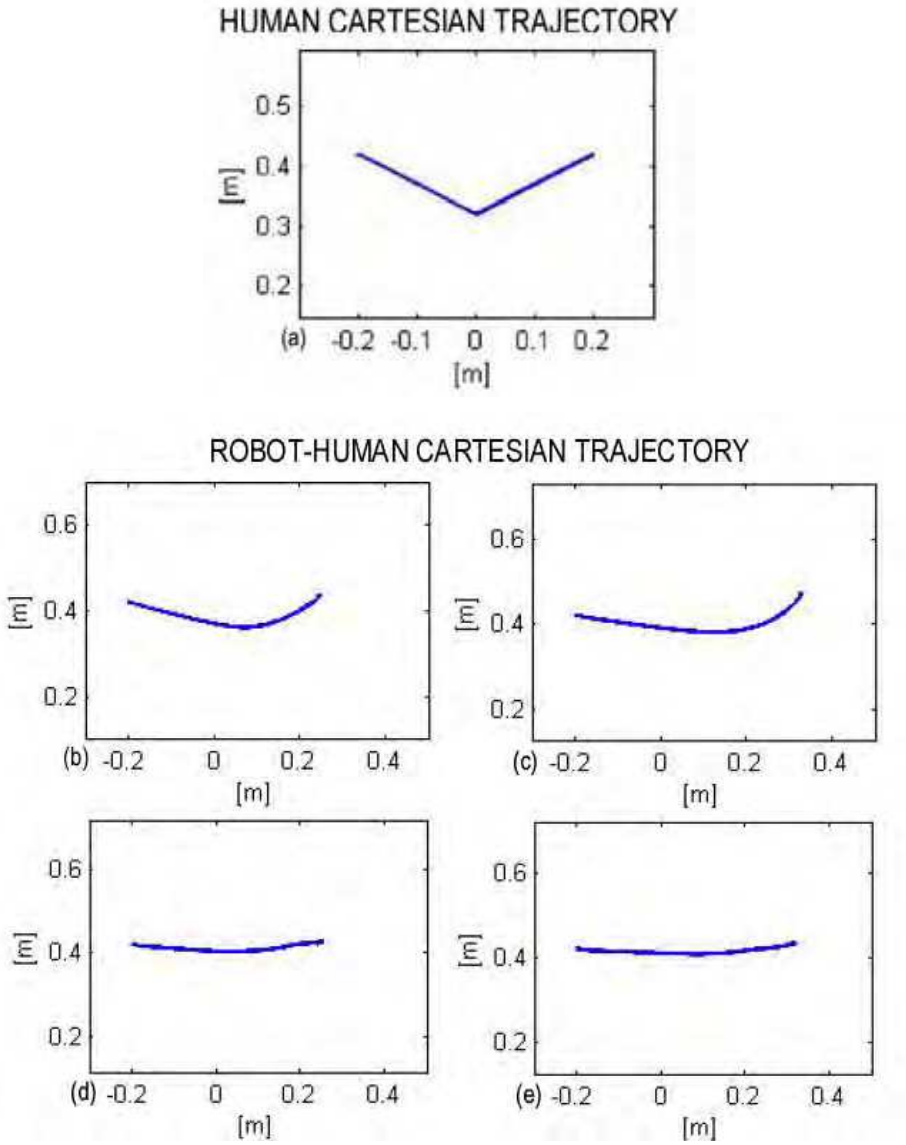

Fig. 15. Pathological trajectory (a) and subject trajectories counterbalanced by the robot for F_{dx} = *5 N* K_y = *100 N/m* (b), F_{dx} = *15 N* K_y = *100 N/m* (c), F_{dx} = *5 N* K_y = *1000 N/m* (d), F_{dx} = *15 N* K_y = *1000 N/m* (e) in case of slight disability.

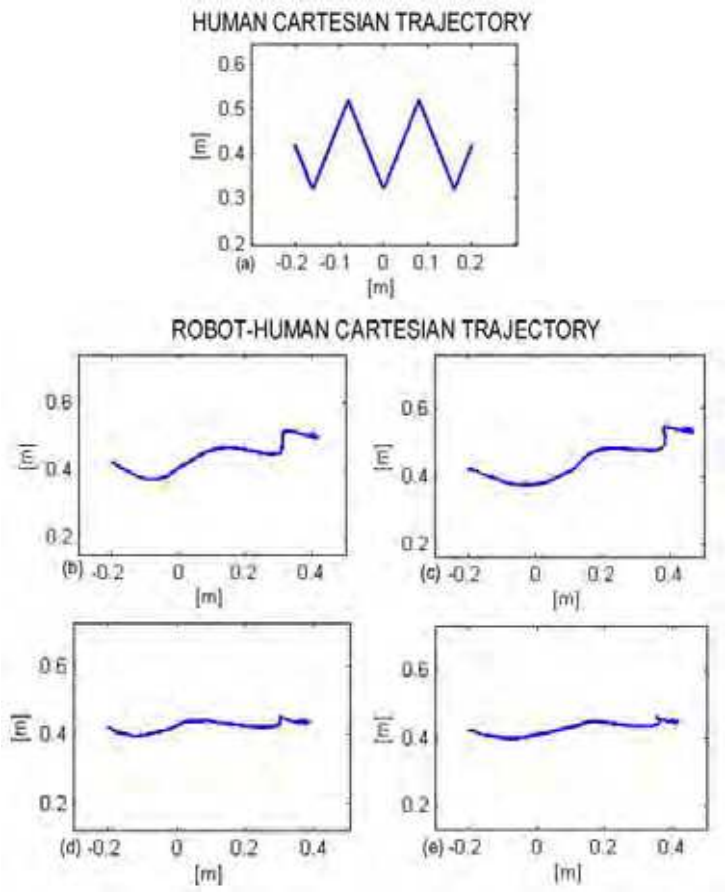

Fig. 16. Pathological trajectory (a) and subject trajectories counterbalanced by the robot for F_{dx} = *30 N* K_y = *100 N/m* (b), F_{dx} = *45 N* K_y = *100 N/m* (c), F_{dx} = *30 N* K_y = *1000 N/m* (d), F_{dx} = *45 N* K_y = *1000 N/m* (e) in case of severe disability.

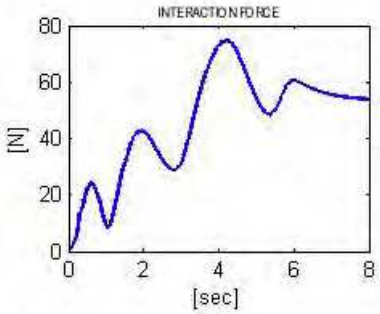

Fig. 17. Interaction force between the robot arm and the patient in case of severe disability and high control parameters (F_{dx} = *45 N*, K_y = *1000 N/m*).

5. Conclusions

In this chapter basic criteria for the design and implementation of interaction control of robotic machines for motor therapy have been briefly introduced and two bio-inspired compliance control laws developed by the authors to address requirements coming from this specific application field have been presented.

The two control laws are named the *coactivation-based compliance control in the joint space* and the *torque-dependent compliance control in the joint space*, respectively. They try to overcome limitations of the traditional interaction control by taking inspiration from biological motor control, with particular attention to the mechanisms of visco-elastic regulation of the human arm. They basically differ for the strategy of stiffness regulation used to generate a variable proportional gain in the PD control.

The control has been designed to ensure a high level of adaptability to different patient motor capabilities and guarantee the maximum level of safety in the interaction. However, also requirements coming from the theory of robot control, such as simplicity of implementation, low computational burden and functional force regulation have been taken into account.

In order to carry out a preliminary evaluation of control performance, a simulation tool has been purposely developed in MATLAB/Simulink. It allows simulating the dynamics of the MIT-Manus rehabilitation robot coupled with a human arm.

Trials of robot positioning in the free space and in the constrained space have revealed similar performance of the control laws as regards position regulation. However, for force regulation in presence of unexpected constraints the coactivation-based control appears to be less safe than the torque-dependent compliance control, due to the numerous and sharp spikes in the contact/noncontact transitions. This result is enforced by the experimental evidence on a 8-dof robot arm.

Based on these preliminary experimental results, the application of the torque-dependent compliance control in the joint space to rehabilitation motor therapy has been simulated. The simulator in fact can be also used to simulate different levels of disability of the patient interacting with the robot. The results showed that also in presence of severe disability the control system is capable of counterbalancing incorrect movements, with an efficacy dependent on tuning the control parameters.

Future work will be addressed to further investigate performance of the coactivation-based and torque-dependent compliance control by implementing the two control laws on a real operational robotic machine for motor therapy (e.g. the MIT-Manus system) and carrying out clinical trials. Also, the formulation of the control law in the joint space ensures an easy portability of the control law to exoskeletal systems. Thus, an extension and application of the two compliance controls to these types of machines is envisaged in the near future.

6. References

Baldissera, F., Hultborn, H., & Illert, M. (1981). In *Handbook of Physiology, Section 1: The nervous system*, J.M. Brookhart, V.B. Mountcastle, V.S. Brooks, S.R. Geiger (Eds.), vol 2 pp 509–595, American Physiology Society, Bethesda.

Bhushan, N., & Shadmehr, R. (1999). Computational Nature of Human Adaptive Control During Learning of Reaching Movements in Force Fields, *Biological Cybernetics*, Vol. 81, pp. 39–60.

Bicchi, A., & Tonietti, G. (2004). Fast and 'Soft-Arm' Tactics. Dealing With the Safety-Performance Tradeoff in Robot Arms Design and Control, *IEEE Robotics and Automation Magazine*, Vol. 11, pp. 22–33.

Colombo, C., Joerg, M., Schreier, R., & Dietz, V. (2000). Treadmill Training of Paraplegic Patients Using a Robotic Orthosis, *J. Rehabil. Res. Dev.*, Vol. 37, pp. 693–700.

Colombo, G. (2004). Treadmill Training With the Robotic Orthosis 'Lokomat': New Technical Features and Results From Multicenter Trial in Chronic Spinal Cord Injury, *Int. J. Rehabil. Res.*, Vol. 27, pp. 92–93.

Costa, N., Brown, M., & Caldwell, D. G. (2004). A Lower Body Exoskeletal Rehabilitation System, *3rd IARP-IEEE/RAS Joint Workshop on Technical Challenge for Dependable Robots in Human Environments*, Manchester, England.

Fasoli, S. E., Krebs, H. I., Stein, J., Frontera, W. R., & Hogan, N. (2003) Effect of Robotic Therapy on Motor Impairment and Recovery in Chronic Stroke, *Arch. Phys. Med. Rehabil.*, Vol. 84, pp. 477–482.

Formica, D., Zollo, L., & Guglielmelli, E. (2005) Torque-Dependent Compliance Control in the Joint Space of a Cartesian Robotic Machine for Motor Therapy, *9th IEEE International Conference on Rehabilitation Robotics*, Chicago, pp. 341–344.

Formica, D., Zollo L., & Guglielmelli, E. (2006). Torque-Dependent Compliance Control in the Joint Space for Robot-Mediated Motor Therapy, *ASME Journal of Dynamic Systems, Measurement, and Control*, Vol. 128, pp. 152- 158.

Gomi, H., & Kawato, M. (1997). Human arm stiffness and equilibrium-point trajectory during multi-joint movement, *Biological Cybernetics*, Vol. 76, pp. 163–171.

Gomi, H., & Osu, R. (1998). Task-dependent viscoelasticity of human multijoint arm and its spatial characteristics for interaction with environments, *Journal of Neuroscience*, Vol. 18, pp. 8965–8978.

Gomi, H. (1998) Anisotropic stiffness reduction during constrained multijoint arm movement, *20th Annual International of the IEEE Engineering in Medicine and Biology Society*, Vol. 20, No. 5, pp. 2336–2337.

Gorinevsky, D. M., Formalsky, A. M., & Schneider, A. Yu. (1997). *Force Control of Robotics Systems*, CRC Press, Boca Raton.

Hogan, N. (1985). Impedance control: an approach to manipulation, Part I, II, II, *ASME Journal of Dynamic System, Measurement, and Control*, Vol. 107, pp. 1-24.

Hogan, N., Krebs, H. I., Charnnarong, J., Srikrishna, P., & Sharon, A. (1992). MIT-MANUS: A Workstation for Manual Therapy and Training I, *IEEE International Workshop on Robot and Human Communication*, Tokyo.

Katayama, M., & Kawato, M. (1993). Virtual trajectory and stiffness ellipse during multijoint arm movement predicted by neural inverse models, *Biological Cybernetics*, Vol. 69, pp. 353–362.

Katayama, M., Inoue, S., & Kawato, M. (1998). A strategy of motor learning using adjustable parameters for arm movement, *International Conference of the IEEE Engineering in Medicine and Biology Society*, Vol. 20, pp. 2370–2373.

Kazerooni, H., Houpt, P. K., & Sheridan, T. B. (1986). Robust Compliant Motion for Manipulators. Part 1. The Fundamental Concepts of Compliant Motion. Part 2. Design Methods, *IEEE J. Rob. Autom.*, Vol. 2, pp. 83–105.

Khalili, D., & Zomlefer, M. (1988). An intelligent robotic system for rehabilitation of joints and estimation of body segment parameters, *IEEE Transactions on Biomedical Engineering*, Vol. 35, pp. 138-146.

Kiguchi, K., & Fukuda, T. (2004). A 3DOF Exoskeleton for Upper-Limb Motion Assist—Consideration of the Effect of Biarticular Muscles, *2004 IEEE International Conference on Robotics and Automation*, New Orleans, LA, pp. 2424–2429.

Krebs, H. I., Hogan, N., Aisen, M. L., & Volpe, B. T. (1998). Robot-Aided Neurorihabilitation, *IEEE Trans. Rehabil. Eng.*, Vol. 6, pp. 75–87.

Krebs, H. I., Hogan, N., Volpe, B. T., Aisen, M. L., Edelstein, L., & Diels, C. (1999). Overview of Clinical Trials with MIT-MANUS: A Robot-Aided Neuro-Rehabilitation Facility, *Technol. Health Care*, Vol. 7, pp. 419–423.

Krebs, H. I., Volpe, B. T., Aisen, M. L., & Hogan, N. (2000). Increasing Productivity and Quality of Care: Robot-Aided Neuro-Rehabilitation, *J. Rehabil. Res. Dev.*, Vol. 37, pp. 639–652.

Krebs, H. I., Palazzolo, J. J., Dipietro, L., Ferraro, M., Krol, J., Rannekleiv, V., Volpe, B. T., & Hogan, N. (2003). Rehabilitation robotics: performance-based progressive robot-assisted therapy, *Autonomous Robots*, Kluwer Academics, Vol. 15, pp. 7-20.

Lum, P.S., Burgar, C. G., Kenney, D. E., Van der Loos, H. F. (1999). Quan-tification of force abnormalities during passive and active-assisted upper-limb reaching movements in post-stroke hemiparesis, *IEEE Trans. Biomed. Eng.*, vol. 46, pp. 652–662.

Miall, R. C. (1998). Motor Control, Biological and Theoretical, *The Handbook of Brain Theory and Neural Networks*, M. A. Arbib (Ed.), pp. 597–600.

Micera, S., Carrozza, M., Guglielmelli, E., Cappiello, G., Zaccone, F., Freschi, C., Colombo, R., Mazzone, A., Delconte, C., Pisano, F., Minuco, G., & Dario, P. (2005). A Simple Robotic System for Neurorehabilitation, *Adv. Rob.*, Vol. 19, pp. 271–284.

Mussa-Ivaldi, F. A., Hogan, & N., Bizzi, E. (1985). Neural, mechanical, and geometric factors subserving arm posture in humans, *Journal of Neuroscience*, Vol. 5, pp. 2732–2743.

Osu, R., & Gomi, H. (1999). Multijoint muscle regulation mechanism examined by measured human arm stiffness and EMG signals, *Journal of Neurophysiology*, Vol. 81, pp. 1458–1468.

Reinkensmeyer, D. J., Kahn, L. E., Averbuch, M., McKenna-Cole, A., Schmit, B. D., Rymer, W. Z. (2000a). Understanding and treating arm movement impairment after chronic brain injury: Progress with the ARM Guide, *J. Rehabil. Res. Dev.*, vol. 37, pp. 653–662.

Reinkensmeyer, D., Hogan, N., Krebs, H. I., Lehman, S. L., & Lum, P. S. (2000b). Rehabilitators, robots and guides: new tools for neurological rehabilitation, *Biomechanics and neural control of posture and movement*, J. Winters, P. E. Crago (Eds.), Springer-Verlag, pp. 516-534.

Salisbury, J. K. (1980). Active Stiffness Control of a Manipulator in Cartesian Coordinates, *19th IEEE Conference on Decision and Control*, Albuquerque, NM, Vol. 1, pp. 95–100.

Serres, S.J., & Milner, T.E. (1991). Wrist muscle activation patterns and stiffness associated with stable and unstable mechanical loads, *Exp. Brain Res.*, Vol. 86, pp. 451–458.

Siciliano, B., & Villani, L. (1999). *Robot Force Control*, Kluwer, Academic Publishers, Boston.

Zinn, M., Kathib, O., Roth, B., & Salisbury, J. K. (2004). Playing It Safe: A New Actuation Concept for Human-Friendly Robot Design, *IEEE Rob. Autom. Mag.*, Vol. 11, pp. 12–21.

Zollo, L., Siciliano, B., Guglielmelli, E., & Dario, P. (2003). A bio-inspired approach for regulating visco-elastic properties of a robot arm, *IEEE International Conference on Robotics and Automation*, Taipei, Taiwan, pp. 14–19.

Zollo, L., Siciliano, B., Laschi, C., Teti, G., & Dario, P. (2003). An experimental study on compliance control for a redundant personal robot arm, *Robotics and Autonomous Systems*, Vol. 44, pp. 101–129.

Zollo, L., Dipietro, L., Siciliano, B., Guglielmelli, E., & Dario, P. (2005). A bio-inspired approach for regulating and measuring visco-elastic properties of a robot arm, *Journal of Robotic Systems*, Vol. 22(8), pp. 397-419.

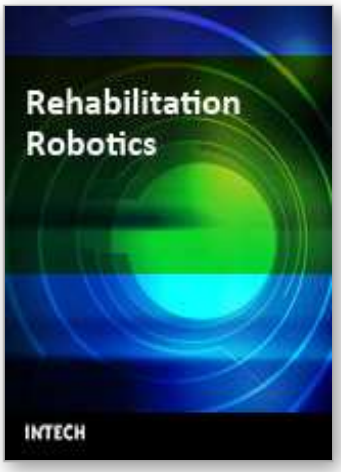

Rehabilitation Robotics

Edited by Sashi S Kommu

ISBN 978-3-902613-04-2

Hard cover, 648 pages

Publisher I-Tech Education and Publishing

Published online 01, August, 2007

Published in print edition August, 2007

The coupling of several areas of the medical field with recent advances in robotic systems has seen a paradigm shift in our approach to selected sectors of medical care, especially over the last decade. Rehabilitation medicine is one such area. The development of advanced robotic systems has ushered with it an exponential number of trials and experiments aimed at optimising restoration of quality of life to those who are physically debilitated. Despite these developments, there remains a paucity in the presentation of these advances in the form of a comprehensive tool. This book was written to present the most recent advances in rehabilitation robotics known to date from the perspective of some of the leading experts in the field and presents an interesting array of developments put into 33 comprehensive chapters. The chapters are presented in a way that the reader will get a seamless impression of the current concepts of optimal modes of both experimental and ap- plicable roles of robotic devices.

How to reference

In order to correctly reference this scholarly work, feel free to copy and paste the following:

Loredana Zollo, Domenico Formica and Eugenio Guglielmelli (2007). Bio-Inspired Interaction Control of Robotic Machines for Motor Therapy, Rehabilitation Robotics, Sashi S Kommu (Ed.), ISBN: 978-3-902613-04-2, InTech, Available from: http://www.intechopen.com/books/rehabilitation_robotics/bio-inspired_interaction_control_of_robotic_machines_for_motor_therapy

INTECH
open science | open minds

InTech Europe
University Campus STeP Ri
Slavka Krautzeka 83/A
51000 Rijeka, Croatia
Phone: +385 (51) 770 447
Fax: +385 (51) 686 166
www.intechopen.com

InTech China
Unit 405, Office Block, Hotel Equatorial Shanghai
No.65, Yan An Road (West), Shanghai, 200040, China
中国上海市延安西路65号上海国际贵都大饭店办公楼405单元
Phone: +86-21-62489820
Fax: +86-21-62489821